Inorganic Chemistry
Cite This: Inorg. Chem. XXXX, XXX, XXX−XXX
Communication
pubs.acs.org/IC

A Gyroidal MOF with Unprecedented Interpenetrating utc-c Network Exhibiting Exceptional Thermal Stability and Ultrahigh CO_2 Affinity

Wei Xu,[†] Yin-Jiang Tang,[†] Lian-Qing Zheng,[†] Jia-Ming Xu,[†] Jian-Zhong Wu,*[,†] Yong-Cong Ou,*[,†] and Ming-Liang Tong[‡]

[†]School of Chemistry, South China Normal University, Guangzhou 510006, China

[‡]MOE Key Laboratory of Bioinorganic and Synthetic Chemistry, School of Chemistry, Sun Yet-Sen University, Guangzhou 501275, China

Supporting Information

ABSTRACT: A zeolite-like gyroidal MOF (denoted as SCNU-1) constructed with Cu ions and 4-(1H-imidazo-[4,5-*f*][1,10]phenanthrolin-2-yl)phenol has a featured interpenetrating uninodal **utc-c** network which is for the first time found in the real structure. Moreover, SCNU-1 exhibits high thermal (>773 K), solvent, and acid/base stabilities; the largest CO_2 affinity, 90 kJ/mol, among the MOFs functionalized with an aromatic hydroxyl group; and excellent CO_2/N_2 selectivity.

Topology is an abstract but aesthetic multidimensional space which can be more effectively understood through assembling specific substances.[1] Being such a complex geometric topology, gyroid (G minimal surface), which was first found by Schoen in a crystallographic cell,[2] has attracted much attention recently not only because it shows potential fantastic photonic, magnetic, and electrochemical properties[3−5] but also because it can be realized by various topologies which have been theoretically calculated[6−8] and summarized in RCSR.[9] It should be noted that although they exist ubiquitously in natural matter,[10−15] such as cell membranes and butterfly wing scales, these structures are referred to only one network, **srs**.[16] Even in artificial structures there are still very few topological networks, for instance, extensively studied zeolites,[17−20] which are concentrated on four nets: **srs**, **gie**, **fcz**, and **ana**. Therefore, constructing new types of topology for gyroidal structures remains important but challenging work.

Carbon dioxide, one of the predominant greenhouse gases, has brought the attention of many researchers to controllable emission and reduction. One effective approach for CO_2 capture[21] is to use porous materials, such as aluminosilicate zeolites, activated carbons, and metal/covalent-organic frameworks (MOFs/COFs). Constructing MOFs with open metal sizes (OMS) and/or functional groups, such as amino and hydroxyl groups, should be a good way to improve the CO_2 affinity.[22−25] In addition, MOFs have been widely investigated in creating new topologies[26−30] due to the multivariate connecting modes of both metal atoms and organic ligands. Recently sporadically reported by Li and other groups,[31−35] gyroidal MOFs show two more geometric networks, **bcs**[32] and **lcs**.[33] It suggests that MOFs should be an optimistic selection for realizing a new prototype of gyroid. However, precise assembly of modifiable frameworks, especially new topological gyroid, is still a great challenge. From a mathematical point of view, discrete minimal patches could be used in constructing a wealth of minimal surfaces.[36] Similarly, assembling MOFs with rigid and planar ligands, which coordinate with metal atoms in certain angles, would be an effective way to target gyroidal products. In recent years, imidazo[4,5-*f*][1,10]phenanthroline (IP) derivative ligands, used to synthesize MOFs by our group,[37,38] were identified as multidentate ligands with a large conjugate surface which should be prospective candidates. To verify the construction strategy and extend the relationship between G minimal surface and adsorption properties, herein we presented a new gyroidal MOF, $[Cu_3(IP\text{-}POH)_2]\cdot NO_3\cdot 9H_2O$, namely, SCNU-1 (SCNU = South China Normal University), under solvothermal conditions by mixing $Cu(NO_3)_2$ with 4-(1H-imidazo[4,5-*f*][1,10]phenanthrolin-2-yl)-phenol (HIP-POH; Scheme S1). Single crystal structural analysis revealed that SCNU-1 is composed of two interpenetrating **utc** networks, which to the best of our knowledge is the first example found in the real structure,[39] with opposite helical channels. This rare gyroidal MOF also showed high thermal stability (>773 K) and excellent water and chemical stabilities. In addition, gas adsorption experiments indicated that SCNU-1 possessed an ultrahigh affinity of carbon dioxide, with an adsorption enthalpy of 90 kJ/mol, which is the largest in the MOFs functionalized with aromatic hydroxyl groups, and excellent CO_2/N_2 selectivity.

SCNU-1 crystallizes in cubic space group $Ia\bar{3}d$ (Table S1). The asymmetric unit contains one and a half Cu^+ atoms, one $IP\text{-}POH^-$ monoanionic ligand, one-half NO_3^- anion, and 4.5 lattice water molecules, which were confirmed via elemental analysis, thermogravimetric analysis (TGA), and IR spectrum (detailed in SI, Figure S1). Obviously, the Cu−N bond lengths, between 1.856(2) and 2.018(2) Å, indicate that Cu^{2+} ions have been reduced to Cu^+ ones, the valences of which were determined by bond valence sum (BVS).[40] As shown in Figure S2, an $IP\text{-}POH^-$ ligand, acting as a "Y-shape" linker, connects three Cu^+ atoms. Interestingly, this coordination type was rarely reported in the structure based on IP derivative

Received: August 20, 2019

DOI: 10.1021/acs.inorgchem.9b02515
Inorg. Chem. XXXX, XXX, XXX−XXX

ligands.[41] The Cu1 atom in tetrahedral geometry is surrounded by four nitrogen atoms from two chelated phenanthroline groups with a dihedral angle of 89.3(4)°, whereas two other cuprous atoms, Cu2 and Cu3, are linearly coordinated with two nitrogen atoms of different imidazole groups. Notably, the Cu3 atom is not coplanar with the linking IP group (torsion angle of Cu3−N4−C13−N3 is 162.1(2)°), while the Cu2 atom and IP group are nearly horizontal (Figure S3). In addition, the dihedral angles of adjacent IP groups, meeting at Cu2 and Cu3 atoms, are 40.4(4)° and 49.6(2)°, respectively, which means that three running IP groups are at a right angle (Figure S4). Accordingly, along the *a*, *b*, and *c* axes, eight such consecutive IP-POH$^-$ ligands and eight 2-coordinated cuprous atoms compose a repeat unit of 4_1 helices, which can shape left-handedness as well as right-handedness and are further connected into a three-dimensional framework via the 4-coordinated Cu1 atoms (Figures 1 and S5). It is noted that the

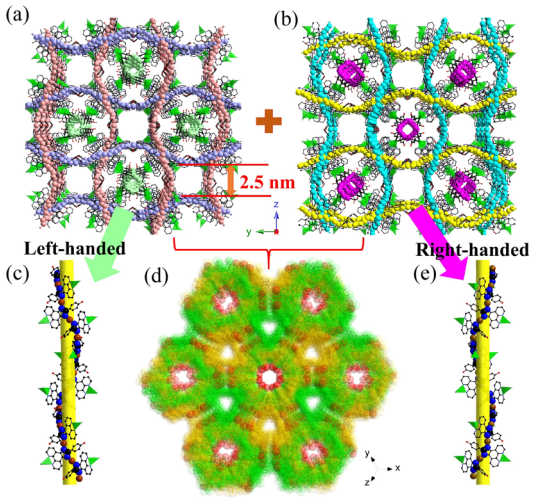

Figure 1. Two 3D frameworks in opposite handedness in SCNU-1 (the left-handed helices in a are colored in light green, brown, and blue, while the right-handed ones in b are highlighted in purple, turquoise, and yellow), composed of pure left-handed (c) and right-handed (e) helices respectively along *a*, *b*, and *c* directions of the coordinate system (Cu1 atoms are shown in green tetrahedra) incorporated in a 2-fold interpenetrated porous structure ((d) space-filling view along (111) direction) in which the hydroxyl groups (red) are fronting the cavity space.

3D structure of SCNU-1, lacking in chiral features, is comprised of two separated interpenetrating frameworks which exhibit opposite handedness originating from homochiral helices and is stabilized through C−H···π interactions (Figure S6). Even though the large square cavity spaces (about 2.5 nm) are reduced by 2-fold interpenetration of the 3D framework, according to the calculation of PLATON,[42] the solvent-accessible volume remains 39 007 Å^3, ca. 54.7% of the cell volume, which includes two kinds of pore cavities, spherical polyhedral cages (inner diameter, 1.8 × 1.6 × 1.4 nm^3) and 1D channels (inner diameter, 0.5 nm; Figures 1d and S7). Notably, all of the aromatic hydroxyl groups of ligands front the cavity space and become partitions of spherical cages, which can be strung together by 1D channels.

As described above, each ligand is linked to three adjacent ones through metal ions, acting as connectors, and in this way the SCNU-1 framework can be simplified into a uninodal 3-connected interpenetrated network (Figure 2a) with a point

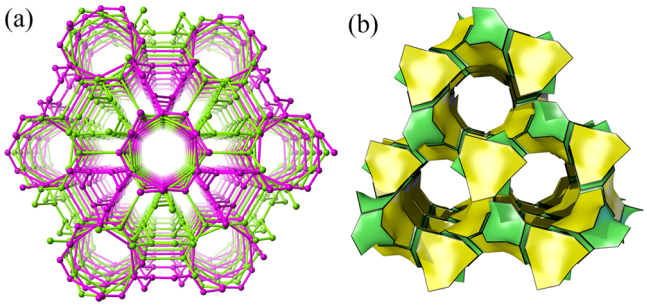

Figure 2. (a) Interpenetrated **utc** networks in SCNU-1 (left-handed and right-handed separated networks are represented in green and purple color, respectively). (b) Tiling representation of half tiles with two kinds of faces colored differently (this half corresponds to the green network in a, while the rest of the tiles are frozen in the empty space).

symbol of $8^2.9$ and a vertex symbol of 8.8.9, which are collected in RCSR as the **utc** nets (single network), and also identified as sphere packing type **3**/**8**/*c***2** and EPINET symbol *sqc***9269**. To the best of our knowledge, SCNU-1 is the first real structure with **utc** networks even though some theoretical studies have been presented.[6−8,39] In addition, as a G minimal surface, the symmetry of the labyrinth graph **utc** is a chiral space group $I4_132$, but for the whole networks in SCNU-1 it is $Ia\bar{3}d$ due to the existence of two opposite chiral **utc** networks. Therefore, the topological symbol for SCNU-1 could be denoted as **utc-c** net (**-c** represented a catenated pair). The tiles in Figure 2b, depicting just half of the tiles (another is shown in Figure S8), illustrates that the **utc-c** network lies on the gyroidal channel, which is separated by the G minimal surface. The construction of a new network can expand the understanding about the relationship between topology and minimal surface.

The stability properties, including thermal and chemical stabilities, have been investigated. The TGA curve of as-synthesized SCNU-1 (Figure 3a) under a nitrogen atmosphere shows a weight loss of 15% before 473 K and 6% more until 573 K, corresponding to the release of nine water molecules and HNO_3, respectively. The PXRD data (Figure S9) of the activated samples at 373 and 573 K were consistent with that of as-synthesized samples, indicating that the crystallinities of SCNU-1 were maintained after a loss of water and HNO_3 molecules. Interestingly, the weight loss was less than 2% until 773 K under a N_2 atmosphere, revealing that the frameworks of SCNU-1 could remain intact at such a high temperature, which was well beyond that of Cu^+-based MOFs, only agreeing with several nonoxidizing metal-based MOFs.[43−46] Comparably, under an oxygen atmosphere, the approximate decomposition temperature of NO_3^- and organic ligands indicated that the Cu−N bonds under a N_2 atmosphere are more stable. Meanwhile, in order to examine the chemical stabilities, activated samples have been immersed into aqueous solutions with different pH values ranging from 2 to 14, common organic solvents at ambient temperature, and boiling water for 24 h, respectively. The resulting PXRD patterns (Figures S10−S12) were the same as that of the as-synthesized material, demonstrating the good maintenance of crystallinity, high acidic and basic stabilities, and excellent resistance to hydrolysis and/or solvation.[47]

The architectural rigidity and consequently the permanent porosity of activated SCNU-1 were unequivocally in evidence via gas sorption analysis. Type I nitrogen sorption isotherm

DOI: 10.1021/acs.inorgchem.9b02515
Inorg. Chem. XXXX, XXX, XXX−XXX

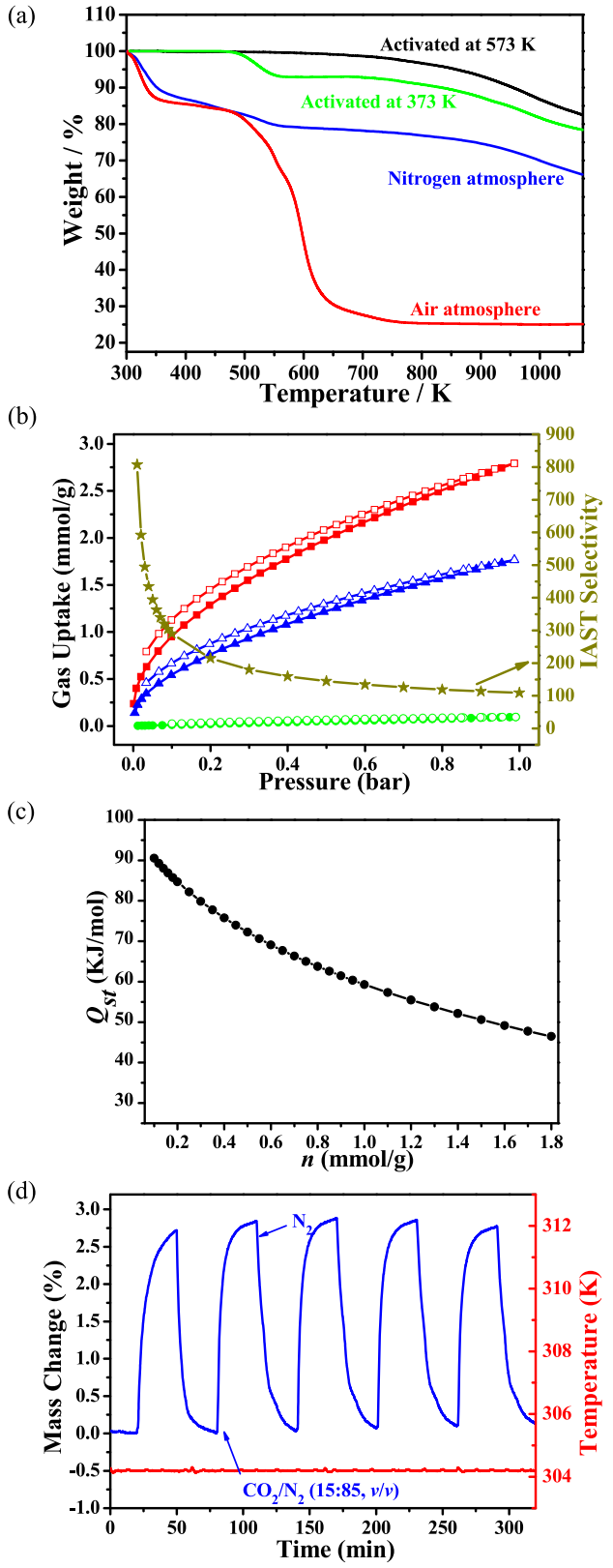

Figure 3. (a) Thermogravimetric plots of as-synthesized sample, activated samples under a N_2 atomsphere, and as-synthesized samples under a O_2 atomsphere. (b) CO_2 adsorption (solid) and desorption (open) isotherms at 273 K (red rectangle) and 298 K (blue triangle), compared with that of N_2 at 298 K (green rhombus), and IAST selectivities of CO_2/N_2 (dark-yellow). (c) CO_2 adsorption enthalpy (Q_{st}) and (d) adsorption−desorption cycling for SCNU-1 between a 15:85 CO_2/N_2 (v/v) flow and a pure N_2 flow at 304 K.

behavior was observed at 77 K for SCNU-1 (Figure S13), which revealed its microporous nature. The Langmuir and BET surface areas based on the data in the low-pressure range (P/P_0 = 0.06−0.25) were 1123 and 774 m^2/g, respectively. The pore volume calculated from the N_2 isotherm was 0.45 $cm^3\ g^{-1}$, in good agreement with the value (0.47 $cm^3\ g^{-1}$) obtained from single-crystal data, which further confirmed the good sample crystallinity and purity.

On the basis of the existence of pore-surface active sites, including 2-coordinated Cu^+ OMS and the hydroxyl group, the CO_2 sorption properties at different temperatures were studied. At 1 bar, SCUN-1 exhibited a CO_2 uptake of 2.75 mmol/g at 273 K and 1.78 mmol/g at 298 K (Figure 3b). Because the isotherms showed relatively large slopes at low pressures, the CO_2 binding affinity was confirmed through the coverage-dependent heat of adsorption of CO_2 (Q_{st}) calculated via both Virial and dual-site Langmuir (DSL) analyses (Figure S14 and 3c). At zero coverage, the maximum adsorption enthalpy of SCUN-1 for the Virial/DSL method reached 78/90 kJ/mol, which is the highest value in hydroxyl-functionalized (Table S3) and amine-functionalized[24,48] MOFs. To the best of our knowledge, the ultrahigh CO_2 affinity surpasses many porous materials containing nucleophilic M−OH groups, such as Zn−OH (71 kJ/mol)[23] and Al−OH (40 kJ/mol),[49] but is only lower than two MOFs[22] containing Co−OH (124 kJ/mol) and Mn−OH (120 kJ/mol). It can be ascribed to the stronger interaction between OMS and CO_2 molecules in SCNU-1, which was calculated through the Adsorption locat0r module in Materials Studio 8.0[50] (Figure S15). Furthermore, the CO_2 affinity can be assigned to the chemisorption interaction, which was probed by *in situ* IR spectra (Figure S16). In a CO_2 atmosphere, new adsorption peaks appeared at 3597, 3625, 3700, and 3725 cm^{-1}, ascribable to the stretching vibration of the H−OCO_2 group. The bands at 2329, 2343, 2353, and 2368 cm^{-1}, red-shifted and blue-shifted from the unperturbed value of the CO_2 asymmetric stretch (2349 cm^{-1}), also confirmed the interactions between CO_2 and hydroxyl groups and OMS, respectively.[51]

The selectivity for adsorption of CO_2 over N_2 is the primary condition for MOFs applicable as carbon dioxide capture materials. To evaluate the potential for separating CO_2/N_2 mixtures, the N_2 sorption isotherm for SCNU-1 was measured at 298 K, which showed uptakes of 0.09 mmol/g at 1 bar, and the CO_2/N_2 selectivity under conditions of a typical composition of flue gas (CO_2/N_2, 15:85) was predicted from the experimental one-component isotherms using the ideal adsorption solution theory (IAST).[52] Due to the strong adsorption sites occupied at low pressure, CO_2/N_2 selectivity of SCNU-1 decreased with increasing pressure (Figure 3b). At 298 K, the CO_2/N_2 selectivities at 1 bar were up to 108, which was comparable with some typical MOFs with OMS and/or hydroxyl groups, such as HKUST-1 (101),[53] UiO-66(Zr)-$(OH)_2$ (105),[54] and Mg-MOF-74 (148).[55]

The regeneration of the CO_2 adsorption−desorption process in SCNU-1 during the gas cycling at 304 K was carried out by TGA with a purge gas swinging between a 15:85 CO_2/N_2 mixture and a pure N_2 flow. About a 2.8 wt % weight change was observed and maintained well over repeated cycles (Figure 3d), indicating that SCNU-1 was able to withstand cyclic exposure to the mixed gas stream and more importantly can be regenerated only by flushing with N_2 at low temperatures.

DOI: 10.1021/acs.inorgchem.9b02515
Inorg. Chem. XXXX, XXX, XXX−XXX

In summary, an interpenetrated gyroidal MOF, SCNU-1, with an unprecedented **utc-c** network has been reported first here and shows not only exceptional thermal stability (>773 K) and high chemical stabilities but also ultrahigh CO_2 binding affinity (90 kJ/mol) and CO_2/N_2 selectivity. These results can provide a new way to understand the relationship between the structure of the minimal surface and properties and should be instructive for designing novel frameworks and discovering good adsorbents for CO_2 separation.

■ ASSOCIATED CONTENT

Supporting Information

The Supporting Information is available free of charge on the ACS Publications website at DOI: 10.1021/acs.inorgchem.9b02515.

Experimental and calculation details and supplementary figures (PDF)

Accession Codes

CCDC 1919463 contains the supplementary crystallographic data for this paper. These data can be obtained free of charge via www.ccdc.cam.ac.uk/data_request/cif, or by emailing data_request@ccdc.cam.ac.uk, or by contacting The Cambridge Crystallographic Data Centre, 12 Union Road, Cambridge CB2 1EZ, UK; fax: +44 1223 336033.

■ AUTHOR INFORMATION

Corresponding Authors

*E-mail: ouyongcong@m.scnu.edu.cn.
*E-mail: wujianzhong@m.scnu.edu.cn.

ORCID

Yong-Cong Ou: 0000-0001-9773-0090
Ming-Liang Tong: 0000-0003-4725-0798

Notes

The authors declare no competing financial interest.

■ ACKNOWLEDGMENTS

This work was supported by NSFC (21401058) and South China Normal University. We thank the staff from the BL17B beamline at Shanghai Synchrotron Radiation Facility (SSRF) for assistance during data collection. We thank Mr. W.-Q. Zhang of Sun Yet-Sen University for gas adsorption and discussion.

■ REFERENCES

(1) Alexandrov, E. V.; Shevchenko, A. P.; Blatov, V. A. Topological databases: why do we need them for design of coordination polymers? *Cryst. Growth Des.* **2019**, *19*, 2604−2614.

(2) Schoen, A. Reflections concerning triply-periodic minimal surfaces. *Interface Focus* **2012**, *2*, 658−668.

(3) Dolan, J. A.; Wilts, B. D.; Vignolini, S.; Baumberg, J. J.; Steiner, U.; Wilkinson, T. D. Optical properties of gyroid structured materials: from photonic crystals to metamaterials. *Adv. Opt. Mater.* **2015**, *3*, 12−32.

(4) Kibsgaard, J.; Chen, Z.; Reinecke, B. N.; Jaramillo, T. F. Engineering the surface structure of MoS_2 to preferentially expose active edge sites for electrocatalysis. *Nat. Mater.* **2012**, *11*, 963−969.

(5) Scherer, M. R. J.; Li, L.; Cunha, P. M. S.; Scherman, O. A.; Steiner, U. Enhanced Electrochromism in Gyroid-Structured Vanadium Pentoxide. *Adv. Mater.* **2012**, *24*, 1217−1221.

(6) Fischer, W. Minimal densities of cubic sphere-packing types. *Acta Crystallogr., Sect. A: Found. Crystallogr.* **2004**, *A60*, 246−249.

(7) Bonneau, C.; Delgado-Friedrichs, O.; O'Keeffe, M.; Yaghi, O. M. Three-periodic nets and tilings: minimal nets. *Acta Crystallogr., Sect. A: Found. Crystallogr.* **2004**, *60*, 517−520.

(8) Ramsden, S. J.; Robins, V.; Hyde, S. T. Three-dimensional Euclidean nets from two-dimensional hyperbolic tilings: kaleidoscopic examples. *Acta Crystallogr., Sect. A: Found. Crystallogr.* **2009**, *A65*, 81−108.

(9) O'Keeffe, M.; Peskov, M. A.; Ramsden, S. J.; Yaghi, O. M. The reticular chemistry structure resource (RCSR) database of, and symbols for, crystal nets. *Acc. Chem. Res.* **2008**, *41*, 1782−1789.

(10) Andersson, S.; Hyde, S. T.; Larsson, K.; Lidin, S. Minimal surfaces and structures: from inorganic and metal crystals to cell membranes and biopolymers. *Chem. Rev.* **1988**, *88*, 221−242.

(11) Wu, L.; Zhang, W.; Zhang, D. Engineering Gyroid-Structured Functional Materials via Templates Discovered in Nature and in the Lab. *Small* **2015**, *11*, 5004−5022.

(12) Han, L.; Che, S. An Overview of Materials with Triply Periodic Minimal Surfaces and Related Geometry: From Biological Structures to Self-Assembled Systems. *Adv. Mater.* **2018**, *30*, 1705708.

(13) Wilts, B. D.; Apeleo Zubiri, B.; Klatt, M. A.; Butz, B.; Fischer, M. G.; Kelly, S. T.; Spiecker, E.; Steiner, U.; Schroder-Turk, G. E. Butterfly gyroid nanostructures as a time-frozen glimpse of intracellular membrane development. *Sci. Adv.* **2017**, *3*, No. e1603119.

(14) Hsueh, H. Y.; Yao, C. T.; Ho, R. M. Well-ordered nanohybrids and nanoporous materials from gyroid block copolymer templates. *Chem. Soc. Rev.* **2015**, *44*, 1974−2018.

(15) Hyde, S. T.; O'Keeffe, M.; Proserpio, D. M. A short history of an elusive yet ubiquitous structure in chemistry, materials, and mathematics. *Angew. Chem., Int. Ed.* **2008**, *47*, 7996−8000.

(16) Goi, E.; Cumming, B. P.; Gu, M. Gyroid "srs" Networks: Photonic Materials Beyond Nature. *Adv. Opt. Mater.* **2018**, *6*, 1800485.

(17) Kresge, C. T.; Leonowicz, M. E.; Roth, W. J.; Vartuli, J. C.; Beck, J. S. Ordered mesoporous molecular sieves synthesized by a liquid-crystal template mechanism. *Nature* **1992**, *359*, 710.

(18) Gier, T. E.; Bu, X.; Feng, P.; Stucky, G. D. Synthesis and organization of zeolite-like materials with three-dimensional helical pores. *Nature* **1998**, *395*, 154.

(19) Zou, X.; Conradsson, T.; Klingstedt, M.; Dadachov, M. S.; O'Keeffe, M. A mesoporous germanium oxide with crystalline pore walls and its chiral derivative. *Nature* **2005**, *437*, 716.

(20) Sun, J.; Bonneau, C.; Cantin, A.; Corma, A.; Diaz-Cabanas, M. J.; Moliner, M.; Zhang, D.; Li, M.; Zou, X. The ITQ-37 mesoporous chiral zeolite. *Nature* **2009**, *458*, 1154.

(21) Sumida, K.; Rogow, D. L.; Mason, J. A.; McDonald, T. M.; Bloch, E. D.; Herm, Z. R.; Bae, T.-H.; Long, J. R. Carbon Dioxide Capture in Metal-Organic Frameworks. *Chem. Rev.* **2012**, *112*, 724−781.

(22) Liao, P.-Q.; Chen, H.; Zhou, D. D.; Liu, S. Y.; He, C. T.; Rui, Z.; Ji, H.; Zhang, J. P.; Chen, X. M. Monodentate hydroxide as a super strong yet reversible active site for CO_2 capture from high-humidity flue gas. *Energy Environ. Sci.* **2015**, *8*, 1011−1016.

(23) Bien, C. E.; Chen, K. K.; Chien, S. C.; Reiner, B. R.; Lin, L. C.; Wade, C. R.; Ho, W. W. Bioinspired Metal−Organic Framework for Trace CO_2 Capture. *J. Am. Chem. Soc.* **2018**, *140*, 12662−12666.

(24) McDonald, T. M.; Lee, W. R.; Mason, J. A.; Wiers, B. M.; Hong, C. S.; Long, J. R. Capture of carbon dioxide from air and flue gas in the alkylamine-appended metal−organic framework mmen-Mg_2(dobpdc). *J. Am. Chem. Soc.* **2012**, *134*, 7056−7065.

(25) Xie, L.-H.; Suh, M. P. High CO_2-Capture Ability of a Porous Organic Polymer Bifunctionalized with Carboxy and Triazole Groups. *Chem. - Eur. J.* **2013**, *19*, 11590−11597.

(26) Chen, B.; Eddaoudi, M.; Hyde, S. T.; O'Keeffe, M.; Yaghi, O. M. Interwoven metal-organic framework on a periodic minimal surface with extra-large pores. *Science* **2001**, *291*, 1021−1023.

(27) Zhang, J.-P.; Zhang, Y.-B.; Lin, J.-B.; Chen, X.-M. Metal azolate frameworks: from crystal engineering to functional materials. *Chem. Rev.* **2012**, *112*, 1001−1033.

DOI: 10.1021/acs.inorgchem.9b02515
Inorg. Chem. XXXX, XXX, XXX−XXX

(28) Zhao, D.; Timmons, D. J.; Yuan, D.; Zhou, H.-C. Tuning the Topology and Functionality of Metal−Organic Frameworks by Ligand Design. *Acc. Chem. Res.* **2011**, *44*, 123−133.
(29) Stock, N.; Biswas, S. Synthesis of metal-organic frameworks (MOFs): routes to various MOF topologies, morphologies, and composites. *Chem. Rev.* **2012**, *112*, 933−969.
(30) Li, M.; Li, D.; O'keeffe, M.; Yaghi, O. M. Topological analysis of metal−organic frameworks with polytopic linkers and/or multiple building units and the minimal transitivity principle. *Chem. Rev.* **2014**, *114*, 1343−1370.
(31) Zhou, X. P.; Li, M.; Liu, J.; Li, D. Gyroidal metal−organic frameworks. *J. Am. Chem. Soc.* **2012**, *134*, 67−70.
(32) Mallik, A. B.; Lee, S.; Lobkovsky, E. B. Three trigonal coordination extended solids with gyroid and lamellar topologies. *Cryst. Growth Des.* **2005**, *5*, 609−616.
(33) Wang, F.; Fu, H. R.; Zhang, J. Homochiral Metal−Organic Framework with Intrinsic Chiral Topology and Helical Channels. *Cryst. Growth Des.* **2015**, *15*, 1568−1571.
(34) Luo, X.; Cao, Y.; Wang, T.; Li, G.; Li, J.; Yang, Y.; Xu, Z.; Zhang, J.; Huo, Q.; Liu, Y.; Eddaoudi, M. Host−Guest Chirality Interplay: A Mutually Induced Formation of a Chiral ZMOF and Its Double-Helix Polymer Guests. *J. Am. Chem. Soc.* **2016**, *138*, 786−789.
(35) Huang, J.; He, Y.; Yao, M. S.; He, J.; Xu, G.; Zeller, M.; Xu, Z. A semiconducting gyroidal metal-sulfur framework for chemiresistive sensing. *J. Mater. Chem. A* **2017**, *5*, 16139−16143.
(36) Karcher, H.; Polthier, K. Construction of triply periodic minimal surfaces. *Philos. Trans. R. Soc., A* **1996**, *354*, 2077−2104.
(37) Zhou, X.; Peng, J. L.; Wen, C. Y.; Liu, Z. Y.; Wang, X. H.; Wu, J. Z.; Ou, Y. C. Tuning the structure and Zn(ii) sensing of lanthanide complexes with two phenylimidazophenanthrolines by acetonitrile hydrolysis. *CrystEngComm* **2017**, *19*, 6533−6539.
(38) Lu, Y. N.; Peng, J. L.; Zhou, X.; Wu, J. Z.; Ou, Y. C.; Cai, Y. P. Rapid naked-eye luminescence detection of carbonate ion through acetonitrile hydrolysis induced europium complexes. *CrystEngComm* **2018**, *20*, 7574−7581.
(39) Hyde, S. T.; O'Keeffe, M. At sixes and sevens, and eights, and nines: schwarzites p3, p= 7, 8, 9. *Struct. Chem.* **2017**, *28*, 113−121.
(40) Brown, I. D. Recent developments in the methods and applications of the bond valence model. *Chem. Rev.* **2009**, *109*, 6858−6919.
(41) Huang, M. M.; Guo, Y. M.; Shi, Y.; Zhao, L.; Niu, Y. W.; Shi, Y.; Li, X. L. Luminescent agostic Cu(I) complexes containing both trigonal planar and tetrahedral coordination modes. *Inorg. Chim. Acta* **2017**, *457*, 107−115.
(42) Spek, A. L. Structure validation in chemical crystallography. *Acta Crystallogr., Sect. D: Biol. Crystallogr.* **2009**, *D65*, 148−155.
(43) Park, K. S.; Ni, Z.; Côté, A. P.; Choi, J. Y.; Huang, R.; Uribe-Romo, F. J.; Chae, H. K.; O'Keeffe, M.; Yaghi, O. M. Exceptional chemical and thermal stability of zeolitic imidazolate frameworks. *Proc. Natl. Acad. Sci. U. S. A.* **2006**, *103*, 10186−10191.
(44) Cavka, J. H.; Jakobsen, S.; Olsbye, U.; Guillou, N.; Lamberti, C.; Bordiga, S.; Lillerud, K. P. A new zirconium inorganic building brick forming metal organic frameworks with exceptional stability. *J. Am. Chem. Soc.* **2008**, *130*, 13850−13851.
(45) Qi, X. L.; Lin, R. B.; Chen, Q.; Lin, J. B.; Zhang, J. P.; Chen, X. M. A flexible metal azolate framework with drastic luminescence response toward solvent vapors and carbon dioxide. *Chem. Sci.* **2011**, *2*, 2214−2218.
(46) Xie, L.-H.; Liu, X.-M.; He, T.; Li, J.-R. Metal-Organic Frameworks for the Capture of Trace Aromatic Volatile Organic Compounds. *Chem.* **2018**, *4*, 1911−1927.
(47) Burtch, N. C.; Jasuja, H.; Walton, K. S. Water Stability and Adsorption in Metal−Organic Frameworks. *Chem. Rev.* **2014**, *114*, 10575−10612.
(48) McDonald, T. M.; D'Alessandro, D. M.; Krishna, R.; Long, J. R. Enhanced carbon dioxide capture upon incorporation of N,N′-dimethylethylenediamine in the metal-organic framework CuBTTri. *Chem. Sci.* **2011**, *2*, 2022−2028.
(49) Li, L.; da Silva, I.; Kolokolov, D. I.; Han, X.; Li, J.; Smith, G.; Cheng, Y.; Daemen, L. L.; Morris, C. G.; Godfrey, H. G. W.; Jacques, N. M.; Zhang, X.; Manuel, P.; Frogley, M. D.; Murray, C. A.; Ramirez-Cuesta, A. J.; Cinque, G.; Tang, C. C.; Stepanov, A. G.; Yang, S.; Schroder, M. Post-synthetic modulation of the charge distribution in a metal−organic framework for optimal binding of carbon dioxide and sulfur dioxide. *Chem. Sci.* **2019**, *10*, 1472−1482.
(50) Cerný, V. Thermodynamical approach to the travelling salesman problem: An efficient simulation algorithm. *J. Optim. Theor. Appl.* **1985**, *45*, 41−51.
(51) Li, B.; Zhang, Z.; Li, Y.; Yao, K.; Zhu, Y.; Deng, Z.; Yang, F.; Zhou, X.; Li, G.; Wu, H.; Nijem, N.; Chabal, Y. J.; Lai, Z.; Han, Y.; Shi, Z.; Feng, S.; Li, J. Enhanced binding affinity, remarkable selectivity, and high capacity of CO_2 by dual functionalization of a rht-type metal−organic framework. *Angew. Chem., Int. Ed.* **2012**, *51*, 1412−1415.
(52) Myers, A. L.; Prausnitz, J. M. Thermodynamics of mixed-gas adsorption. *AIChE J.* **1965**, *11*, 121−127.
(53) Liang, Z.; Marshall, M.; Chaffee, A. L. CO_2 adsorption-based separation by metal organic framework (Cu-BTC) versus zeolite (13X). *Energy Fuels* **2009**, *23*, 2785−2789.
(54) Hu, Z.; Wang, Y.; Farooq, S.; Zhao, D. A highly stable metal-organic framework with optimum aperture size for CO_2 capture. *AIChE J.* **2017**, *63*, 4103−4114.
(55) Mason, J. A.; Sumida, K.; Herm, Z. R.; Krishna, R.; Long, J. R. Evaluating metal−organic frameworks for post-combustion carbon dioxide capture via temperature swing adsorption. *Energy Environ. Sci.* **2011**, *4*, 3030−3040.

DOI: 10.1021/acs.inorgchem.9b02515
Inorg. Chem. XXXX, XXX, XXX−XXX